New Journal of Physics
The open access journal at the forefront of physics

Deutsche Physikalische Gesellschaft DPG IOP Institute of Physics

OPEN ACCESS

Electrodynamic structure of charged dust clouds in the earth's middle atmosphere

To cite this article: W A Scales and G Ganguli 2004 *New J. Phys.* **6** 12

View the article online for updates and enhancements.

You may also like

- Charged dust phenomena in the near-Earth space environment
W A Scales and A Mahmoudian
- Nanostructured lipid carrier potentiated oral delivery of raloxifene for breast cancer treatment
Nimrit Kaur Soni, LJ Sonali, Archu Singh et al.
- Combined strategies of apomorphine diester prodrugs and nanostructured lipid carriers for efficient brain targeting
Kuo-Sheng Liu, Chih-Jen Wen, Tzu-Chen Yen et al.

This content was downloaded from IP address 194.95.157.36 on 24/01/2025 at 09:24

New Journal of Physics
An Institute of Physics and Deutsche Physikalische Gesellschaft Journal

Electrodynamic structure of charged dust clouds in the earth's middle atmosphere

W A Scales[1] **and G Ganguli**[2]

[1] Bradley Department of Electrical and Computer Engineering, Virginia Polytechnic Institute and State University, Blacksburg, VA 24061-0111, USA
[2] Plasma Physics Division, Naval Research Laboratory, Washington, DC 20375-5346, USA
E-mail: wscales@vt.edu

New Journal of Physics **6** (2004) 12
Received 20 February 2003
Published 30 January 2004
Online at http://www.njp.org/ (DOI: 10.1088/1367-2630/6/1/012)

Abstract. Noctilucent clouds (NLCs) and polar mesospheric summer echoes (PMSEs) are two phenomena at the forefront of near-earth space science. NLCs are high-altitude clouds in the earth's mesosphere that are formed from visible aerosol particles. The occurrence rate of NLCs over time is believed to have profound implications on global climate change. NLCs are often associated with PMSEs which are strong 50 MHz–1.3 GHz radar echoes from mesospheric electron irregularities. Therefore, PMSEs may be an important remote-sensing diagnostic for the evolution of NLCs and the earth's middle atmosphere in general. The electron irregularities that produce PMSEs are generally believed to result from charging of electrons onto subvisible aerosol irregularities, the source of which is currently a debated issue. Neutral air turbulence has long been considered a primary source of the irregularities. However, there are clearly fundamental characteristics of the irregularities in past and recent observations that cannot be explained by neutral air turbulence and most probably involve plasma processes. This work considers the latter mechanism and the possibility of production of aerosol irregularities in the boundary region between the charged aerosol layer and the background mesospheric plasma. First a model for investigating the electrodynamics of this boundary layer is described. This model indicates that plasma flows are expected to exist in the electrodynamic equilibrium. An initial assessment of the possible role of these plasma flows in producing irregularities that may ultimately result in PMSEs is provided.

PII: S1367-2630(04)59978-0
© IOP Publishing Ltd and Deutsche Physikalische Gesellschaft

Contents

1. Introduction

The summer polar mesosphere is one of the most intriguing regions in the earth's middle atmosphere for scientific study. It exhibits a rich variety of physical processes that are fundamentally important to middle atmospheric evolution and dynamics but are currently not well understood. Two phenomena that have received intense experimental and theoretical investigation over the last two decades are polar mesospheric summer echoes (PMSEs) and noctilucent clouds (NLCs) [1, 2]. PMSEs are strong radar echoes that were first observed in the late 1970s [3, 4] and are in the 50 MHz–1.3 GHz frequency range. PMSEs are the result of Bragg scattering from mesospheric electron irregularities. The electron irregularities result from charging of electrons onto subvisible aerosol particles (∼10 nm) produced from ice in the earth's mesosphere since the altitude region between 80 and 90 km is the coldest in the atmosphere. These electron irregularities are believed to be long-lived due to the reduced electron diffusivity caused by the presence of the relatively heavy aerosols [5]. NLCs are formed primarily from larger (∼50 nm) visible aerosol particles and are often observed slightly below the PMSE generation region altitude. Therefore, PMSEs may be a crucial remote-sensing diagnostic for interpreting the creation, evolution and dynamics of NLCs. Since the occurrence rate of NLCs has possibly been increasing since their discovery in 1885, they are believed to be an important indicator of global climate changes on earth. Therefore, the study and understanding of PMSEs and NLCs has become a problem at the forefront of near-earth space science.

Development of theories to explain PMSEs and their relationship with NLCs has been quite challenging. This is true because of the complex nature of the constituents and electrodynamics in the generation region. There is a complex mixture of electrons and ions as well as charged aerosols. Also, these are intimately coupled with the background neutral gas dynamics due to the high collisionality with neutrals in this altitude region. A central issue is the production of irregularities in the aerosol density that ultimately lead to the electron irregularities that produce the radar echoes. These aerosol irregularities have been directly observed to have metre-scale variations [6]. Recently [7], it has been reported that there is considerable statistical evidence that neutral air turbulence is responsible for producing these aerosol irregularities. The slow decay time of these aerosol irregularities, due to their large mass, may provide long-lived electron irregularities even after the generating neutral air turbulence has died away [8]. However, there are characteristics of the irregularities that cannot be explained with neutral air turbulence and this has prompted a number of investigators to consider plasma mechanisms (see e.g. [9]–[11]).

A recent example is an experimental observation which clearly shows ac electric fields associated with PMSEs which cannot be explained with neutral air turbulence [12]. This provides further evidence that PMSEs are most probably generated by several different physical processes, and neutral air turbulence and plasma processes as generation mechanisms are not expected to be mutually exclusive.

This work considers a mechanism that may produce aerosol irregularities through unstable plasma waves. These aerosol irregularities ultimately produce the electron irregularities which may result in PMSEs. A feature often, but not always, associated with PMSEs is the so-called electron 'bite-out' which is a region of reduction in electron density and is taken as a clear indication of charging of electrons onto the aerosols. This region of electron reduction can also be taken as an indication of a relatively sharp boundary between the background plasma region of primarily ions and electrons and a dusty plasma region with electrons, ions and also a significant number density of subvisible charged aerosols. This region will be referred to as the charged dust cloud boundary layer in the present work. Plasma boundaries have, in general, been shown to provide free energy for the generation of plasma irregularities [13, 14]. Even though this is the case, this line of investigation associated with PMSE generation has not been pursued in the past. Indeed, recently, there is clear evidence of enhanced ac plasma wave activity in this boundary layer during simultaneous rocket, radar and lidar measurements [12, 15].

The object of this work is to first consider the free energy that may reside in the charged dust cloud boundary layer by first studying the equilibrium electrodynamics. The organization of the paper is as follows. The next section will consider a model to investigate the equilibrium structure of the charged dust cloud boundary layer. The following section describes results of this model and provides a discussion of possible irregularity generation mechanisms. Finally, conclusions will be provided. An important final note on nomenclature should be mentioned here to avoid confusion. The terms 'aerosols' and 'dust' will be used more or less interchangeably. In many works on NLCs, the term 'dust' is used to describe the uncharged smoke particles of meteoric origin in the mesosphere described by the Hunten ablation model [16]. The aerosol particles are water crystals (ice) that nucleate on these meteoric dust particles or also possibly water cluster ions: the particles growing to visible size by condensation and coagulation are visible as NLCs. Other works have considered the charged aerosol region most appropriately as a dusty plasma which is the convention that will be adhered to here.

2. Charged dust cloud boundary layer model

In situ measurements have shown that in the altitude region where subvisible dust exists, there are often reductions in mesospheric electron density commonly referred to as electron 'bite-outs'. These density structures are also often associated with PMSEs and may extend several kilometers in altitude. The electron density reductions are assumed to be formed by electron attachment onto the dust. This attachment is primarily due to the charging process of the flux of thermal electrons and ions onto the dust. The electron reductions can be of the order of 90% or more and the gradient scale lengths on the edges of these density structures may be of the order of tens of metres or less. Therefore, the edge of the charged dust cloud is essentially a boundary between the background ambient plasma of ions and electrons and the region which contains ions, electrons and also heavy charged dust. The dust particle size is of the order of 10 nm. Therefore, the dust typically carries no more than a few negative charges although observations do exist of positive

dust [17, 18]. Previous works have not considered the details of the electrodynamic equilibrium of this boundary layer and the possiblity of free-energy sources for the production of plasma irregularities in the boundary that may lead to PMSEs. The model that is proposed here currently is an admittedly simplified one; however, it is believed to provide the essence of processes in the equilibrium boundary layer.

The ions in the model are described by plasma fluid equations. The ion density is described by the continuity equation

$$\frac{\partial n_\mathrm{i}}{\partial t} + \frac{\partial}{\partial x}(n_\mathrm{i} v_\mathrm{i}) = P_\mathrm{i} + L_\mathrm{i} + \left.\frac{\mathrm{d}n_\mathrm{i}}{\mathrm{d}t}\right|_{\mathrm{charging}}. \tag{1}$$

Here P_i denotes the production of ions by photoionization and L_i denotes the ion loss due to dissociative recombination. This loss term is described by $L_\mathrm{i} = \alpha n_\mathrm{e} n_\mathrm{i}$ where α is the recombination coefficient and n_e is the electron density. The term $\mathrm{d}n_\mathrm{i}/\mathrm{d}t|_{\mathrm{charging}}$ denotes the ion loss due to the ion flux onto the dust. Neglecting inertial effects, the ion velocity is given by the momentum equation as

$$v_\mathrm{i} = \frac{1}{\nu_\mathrm{in}}\left(\frac{q_\mathrm{i}}{m_\mathrm{i}}E - \frac{KT_\mathrm{i}}{m_\mathrm{i}}\frac{\partial}{\partial x}(\log n_\mathrm{i})\right), \tag{2}$$

where q_i, m_i and T_i are the ion charge, mass and temperature, and ν_in is the ion-neutral collision frequency. Also, K is Boltzmann's constant. The electrostatic field is denoted by E.

The dust is modelled with the standard particle-in-cell (PIC) method [19]. Each dust particle is taken to have time-varying charge $Q_\mathrm{d}(t)$. A distribution of masses is also allowed. The dust charge is determined from the standard continuous charging model which is given by [20]

$$\frac{\mathrm{d}Q_\mathrm{d}}{\mathrm{d}t} = I_\mathrm{e} + I_\mathrm{i} + I_\mathrm{p}, \tag{3}$$

where I_e and I_i are the currents onto each individual dust particle by electron and ion flux and I_p is the photoemission current. For negatively charged dust, which will primarily be considered, these currents are given by

$$I_\mathrm{e} = \sqrt{8\pi} r_\mathrm{d}^2 q_\mathrm{e} n_\mathrm{e} v_\mathrm{te} \exp(-q_\mathrm{e}\phi_\mathrm{d}/KT_\mathrm{e}), \tag{4}$$

$$I_\mathrm{i} = \sqrt{8\pi} r_\mathrm{d}^2 q_\mathrm{i} n_\mathrm{i} v_\mathrm{ti}(1 - q_\mathrm{i}\phi_\mathrm{d}/KT_\mathrm{i}) \tag{5}$$

and

$$I_\mathrm{p} = -\pi r_\mathrm{d}^2 q_\mathrm{e} J_\mathrm{p} Q_\mathrm{ab} Y_\mathrm{p} \exp(q_\mathrm{e}\phi_\mathrm{d}/KT_\mathrm{p}). \tag{6}$$

Here, r_d is the dust radius, $v_\mathrm{te,i}$ the electron (ion) thermal velocity and ϕ_d the dust floating potential. This potential may be related to the number of charges on the dust Z_d as well as the dust radius r_d by

$$Z_\mathrm{d} = \frac{4\pi\epsilon_0 r_\mathrm{d}\phi_\mathrm{d}}{q_\mathrm{e}}, \tag{7}$$

where ϵ_0 is the free-space permitivity. Also, J_p, Q_{ab}, Y_p and T_p are the photon flux, photon absorption efficiency, photoelectron yield and average photoelectron temperature. The collision of charged dust with neutrals is implemented by using a Langevin method [21] and the dust-neutral collision frequency is denoted by ν_{dn}. The initially uncharged dust is supposed to have density given by

$$n_d(x) = \frac{n_{d0}}{2}(1 - \tanh((x - x_0)/\ell)), \tag{8}$$

where n_{d0} is the background neutral dust density, x_0 the location of the centre of the boundary, and ℓ the scale length of the boundary.

The electron density is determined from quasi-neutrality

$$n_e(x) = n_i(x) - \rho_d(x)/e, \tag{9}$$

where ρ_d is the dust charge density and e the unit charge. The electron velocity is described by the momentum equation

$$v_e = \frac{1}{\nu_{en}}\left(\frac{q_e}{m_e}E - \frac{KT_e}{m_e}\frac{\partial}{\partial x}(\log n_e)\right), \tag{10}$$

where all quantities are analogous to those for the ions. The electrostatic field is calculated from the condition of zero currents often used in ionospheric plasmas:

$$J_T = q_e n_e \boldsymbol{v}_e + q_i n_i \boldsymbol{v}_i + J_d = 0, \tag{11}$$

where J_T is the total current density of ions, electrons and dust and J_d the dust current density calculated from the simulation dust particles. Substituting the previous expressions for the electron and ion velocities into equation (11), the electrostatic field can be calculated as

$$E = \left(\frac{q_e KT_e}{m_e \nu_{en}}\frac{\partial n_e}{\partial x} + \frac{q_i KT_i}{m_i \nu_{in}}\frac{\partial n_i}{\partial x} - J_d\right) \Big/ \left(\frac{q_e^2}{m_e \nu_{en}}n_e + \frac{q_i^2}{m_i \nu_{in}}n_i\right). \tag{12}$$

It should be noted that since $m_d \gg m_i \gg m_e$, to a good approximation,

$$E \approx \frac{KT_e}{q_e}\frac{\partial}{\partial x}\log n_e, \tag{13}$$

which is a description of Boltzmann behaviour for the electrons.

The model just described above is essentially an extension of the model of Hill [22], which has been used by other investigators in studying irregularities associated with PMSEs [23]. In the case here, chemistry and charging processes as well as diffusion have been included which have not been used extensively until very recently [8]. The charging model here is a continuous one. Owing to the relatively small size of the dust grains ($r_d \sim 10\,\text{nm}$), they are expected to carry no more than a few charges. Previous works involving dust charging in the mesosphere [8, 24, 25] have utilized discrete charging models based on the work of Natanson [26]. The continuous charging model used here is based on the orbital-motion-limited (OML) approach [27, 28]. Since the dust here is modelled with the PIC technique in which each simulation particle represents a large number of actual dust particles, a continuous charging model will

ultimately provide the evolution of the average spatial dust charge which is not unreasonable. Discrete charging can be implemented within the framework of this model in a straightforward manner; however, this is not expected to produce qualitative changes in the results to be presented. The use of the PIC technique to model the dust is expected to have significant advantages in considering the temporal evolution of dust irregularities (e.g. [21]) which will be the subject of future investigations. The current investigation, which does not require dust dynamics, will be used as a reference for this planned future work.

3. Results

The model described in the previous section was used to investigate the electrodynamic equilibrium of the charged dust cloud boundary layer. Initially, the electron and ion densities are taken to be uniform and equal $n_{e0} = n_{i0} = n_0$. The production and loss terms, P_i and L_i, are balanced to sustain a constant value of background plasma density. This of course implies $P_i = \alpha n_0^2$. The dust is allowed to charge as described by equation (3) and the system is then allowed to temporally evolve into an equilibrium state. The electrodynamic equilibrium is investigated for a variation of two primary parameters. This first is the relative density of uncharged dust to the background plasma density n_{d0}/n_{e0}. The second is the equilibrium dust grain charge Z_{eq} which may be determined from equation (7) by calculating the equilibrium floating potential ϕ_{eq}. ϕ_{eq} is calculated from charging equilibrium $\mathrm{d}Q_d/\mathrm{d}t = 0$ in equation (3). Of course, from (7), Z_{eq} is directly related to the dust radius r_d. Again, for the present investigation, the dust is assumed to be immobile. For simplicity, in all the results to be described, the dust is taken to charge negatively and have a uniform radius r_d, or equivalently, mass. Photoemission and electron precipitation effects are also neglected. Since the electron flux onto the dust initially dominates, the initial charging period for a neutral dust grain can be approximated from equation (4) as

$$\tau_{chg} \approx \frac{1}{r_d^2 n_e v_{te}}. \tag{14}$$

For values typical of the mesosphere, $n_0 \sim 10^{10}\,\mathrm{m}^{-3}$ and $T_e = 150\,\mathrm{K}$, τ_{chg} is of the order of 1 s. From the equilibrium condition, the photoionization rate is $1/\alpha n_0$ and is of the order of 100 s.

Other relevant background plasma parameters used are chosen to be typical of the mesosphere at an altitude of 85–90 km and are as follows. The electron neutral collision frequency to electron plasma frequency ratio $\nu_{en}/\omega_{pe} \approx 1$. The ion neutral collision frequency to ion plasma frequency ratio $\nu_{in}/\omega_{pi} \approx 1$. The electron temperature to ion temperature ratio $T_e/T_i = 1$. The system length is several $1000\lambda_{Di}$, where λ_{Di} is the Debye length in the ambient ions. This corresponds to a charge dust cloud boundary layer size of tens of metres.

3.1. Equilibrium structure

Figure 1 shows the temporal evolution of the average charge on the dust and the electrostatic field energy E_F (in arbitrary units). The value of $n_{d0}/n_{e0} = 0.5$ and $Z_{eq} = -2$. It can be seen that the dust initially charges negatively and eventually approaches an equilibrium state after time $t/\tau_{chg} = 75$ when the dust grain ion current becomes significant compared with the dust grain electron current. Physically, the charge equilibrium implies the currents in equation (3)

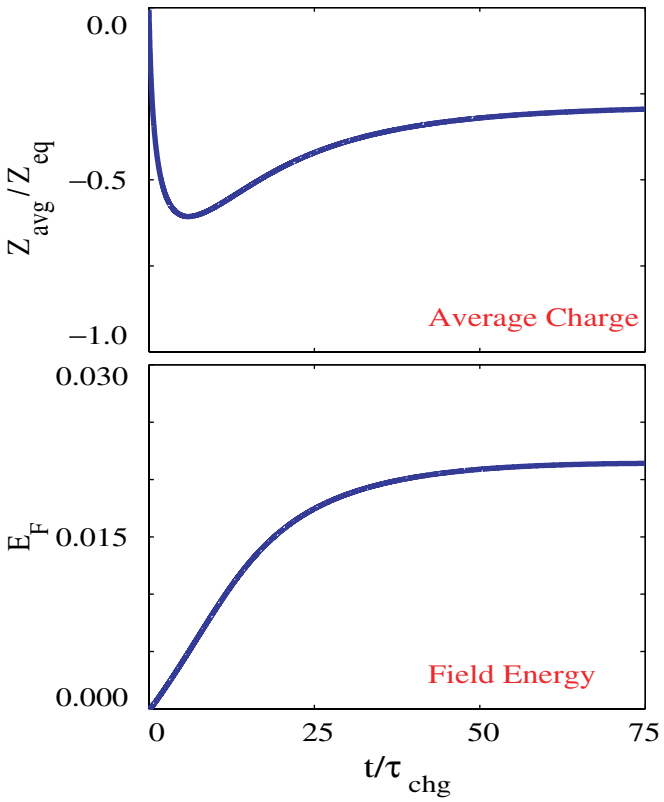

Figure 1. Temporal evolution of the average dust charge and electric field energy (arbitrary units) for the model of section 2. Note initial negative dust charging and growth of electric field energy. The system reaches a steady state after $t/\tau_{\mathrm{chg}} = 75$.

are balanced. Associated with the dust charging is the production of an electric field in the boundary layer. The electric field is ambipolar in nature and develops in response to the diffusion of electrons and ions into the plasma depletion in the presence of the heavy dust particles. This field is directed into the dust cloud ($-\hat{\boldsymbol{x}}$) for the parameters under consideration. This electric field reaches a steady-state value at the same time as the dust charge does. Therefore, the dust charging can be seen to be crucial in producing the electric field which may serve as a free-energy source for irregularities in the boundary layer. It should be noted that strong vertical electric fields have been postulated to exist in the region around NLCs [29]. There has been one rocket observation of a large ($\mathrm{V\,m^{-1}}$) electric field that was highly sheared near a NLC [30]. This report has been somewhat controversial since some recent [31] and previous [32, 33] observations have shown possibly enhanced but smaller ($\mathrm{mV\,m^{-1}}$) dc electric fields near the NLC. Clearly further observations are needed. In the case of the current model parameters, this electric field is of the order of $10\,\mathrm{mV\,m^{-1}}$.

Localized steady-state flows in the ions and electrons are associated with this equilibrium electric field. Figure 2 is summary of the electron, ion and dust charge density after the steady state is reached as well as the ion and electron flows v_{di} and v_{de}. The variation of these quantities with increasing ratio of neutral dust density to background plasma density $n_{\mathrm{d0}}/n_{\mathrm{e0}}$ is shown. The three values shown are $n_{\mathrm{d0}}/n_{\mathrm{e0}} = 1/8, 1, 8$; therefore, the equilibrium configuration is shown for neutral dust densities much smaller to but much larger than the background plasma density.

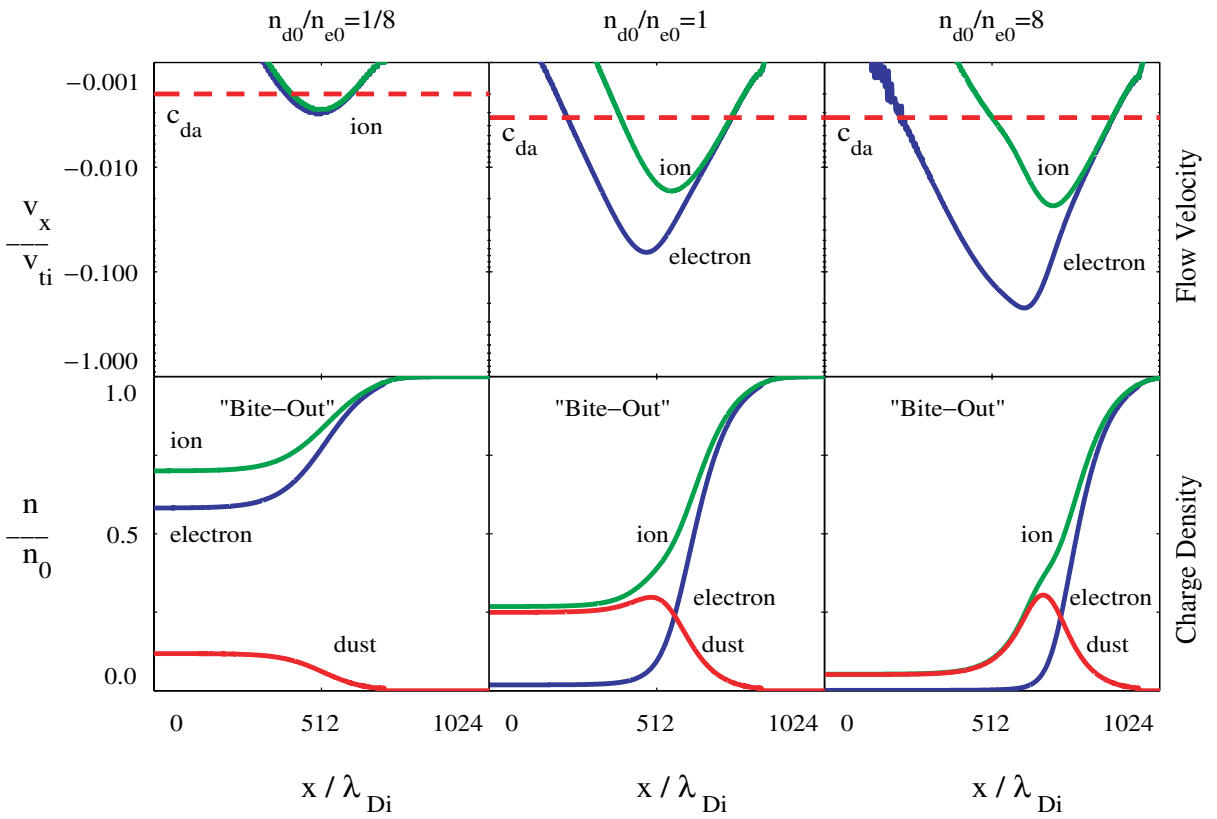

Figure 2. Behaviour of normalized plasma flows and densities in the steady-state charged dust cloud boundary layer with varied neutral dust density n_{d0}/n_{e0} and $Z_{eq} = -1$. Note electron and ion flows which may serve as free energy for irregularity growth are increased with increasing n_{d0}/n_{e0}. These flows exceed the dust acoustic speed c_{da}, denoted by the dotted line. For $n_{d0}/n_{e0} \gg 1$, a prominent maximum exists in the dust charge density in the boundary.

The equilibrium charge $Z_{eq} = -1$ in all three cases. In the low-density case, reduction in both the electron and ion density can be observed with the electron density depletion commonly referred to as an electron 'bite-out'. An ion flow exists, which is about $0.003v_{ti}$. A small electron flow also exists, which is approximately equal to the ion flow. Increasing the background neutral dust density to $n_{d0}/n_{e0} = 1$ increases the depth of the electron 'bite-out' as well as increases the electron and ion flow velocities in the dust cloud boundary. In the case where $n_{d0}/n_{e0} \gg 1$, virtually all electrons in the dust cloud region are gone. The ion density is also quite low. Therefore, very little plasma exists inside the depletion. Most of the dust charge density exists in a localized region in the dust cloud boundary ($x/\lambda_{Di} \sim 640$). Little charge on the dust exists inside the 'bite-out' region. This is in contrast with the other two cases in which the dust charge density is relatively uniform inside the 'bite-out' region. The electron and ion flows are increased as well for $n_{d0}/n_{e0} = 8$. It can also be seen that the electron flow has increased relative to the ion flow. In this case, the ion flow is several per cent of the v_{ti}, i.e. $v_{di} \sim 0.01v_{ti}$. The electron flow is considerably larger than the ion flow and is of the order of $0.1v_{ti}$. The flows do not maximize at the exact same spatial location; however, both maximize in the cloud boundary. It should be

noted that this case with $n_{d0}/n_{e0} \gg 1$ is expected to be atypical of PMSE conditions; however, it may provide predictions of the upper limit on the magnitude of the equilibrium flows. It should be noted that these localized equilibrium flows may be significantly reduced by the nonlinear evolution of irregularities produced by free energy available in the flows. This behaviour is often observed in such plasma configurations [34]. Therefore, the flows provided here should not be considered as steady-state values that would be observed with experimental observations.

An important quantity to compare these flows with is the dust acoustic speed which is given by

$$c_{da} = \omega_{pd}\lambda_{Di} = Z_d v_{ti}\sqrt{\frac{n_d(x)m_i}{n_i(x)m_d}}, \tag{15}$$

where ω_{pd} is the dust plasma frequency, Z_d the dust charge and m_d the dust mass. For typical mesospheric values, c_{da} is of the order $1\,\mathrm{m\,s^{-1}}$. Since the ion and dust densities vary over the cloud region, c_{da} will ultimately have a spatial dependence. The dotted line in figure 2 shows the maximum spatial value of c_{da} for the three cases assuming a typical value of $m_d/m_i = 5 \times 10^4$. In all three cases, the localized flows exceed c_{da}. Increasing the neutral dust density increases the flows relative to c_{da}. The significance of this is the possibility of irregularity generation which will be discussed shortly.

Figure 3 is a plot similar to figure 2, except that the variation of the equilibrium boundary layer with increasing equilibrium charge Z_{eq} is investigated here. Three values are shown, $Z_{eq} = -1$, -2 and -3. This is, of course, equivalent to considering the variation of the equilibrium structure with increasing dust radius r_d as can be seen from (7). In each of these three cases, $n_{d0}/n_{e0} = 0.5$. Increasing Z_{eq} to larger negative values can be seen to deepen the electron depletions; however, the ion depletions become shallower since more charge resides on the dust as expected. The dust charge density shows a more prominent increase in the boundary as Z_{eq} is increased. Increasing Z_{eq} to larger negative values can be seen to increase the electron flow while there is a slight decrease in ion flow. For all three cases, both flows can be observed to significantly exceed c_{da}.

Therefore, to summarize, increasing the neutral dust density or equilibrium dust charge (or equivalently the dust radius) increases the equilibrium electron and ion flows in the charged dust charge boundary. Importantly, these localized flows may exceed the dust acoustic speed c_{da}. Therefore, the boundary flows indicate several possibilities for dust irregularity generation that may ultimately lead to PMSEs. These will now be investigated.

3.2. Irregularity generation

It is evident that the boundary layer is quite inhomogenous from figures 2 and 3; however, a simplified analysis will be provided here to initially investigate several possibilities for irregularity generation. A simple local linear analysis will be considered consisting of electrons and ions drifting relative to the dust. The linear dispersion relation for the irregularity frequency ω and wavenumber k_x in a plasma consisting of electrons, ions and charged dust may be written using standard thermal plasma instability theory [35] as

$$1 + \chi_e + \chi_i + \chi_d = 0, \tag{16}$$

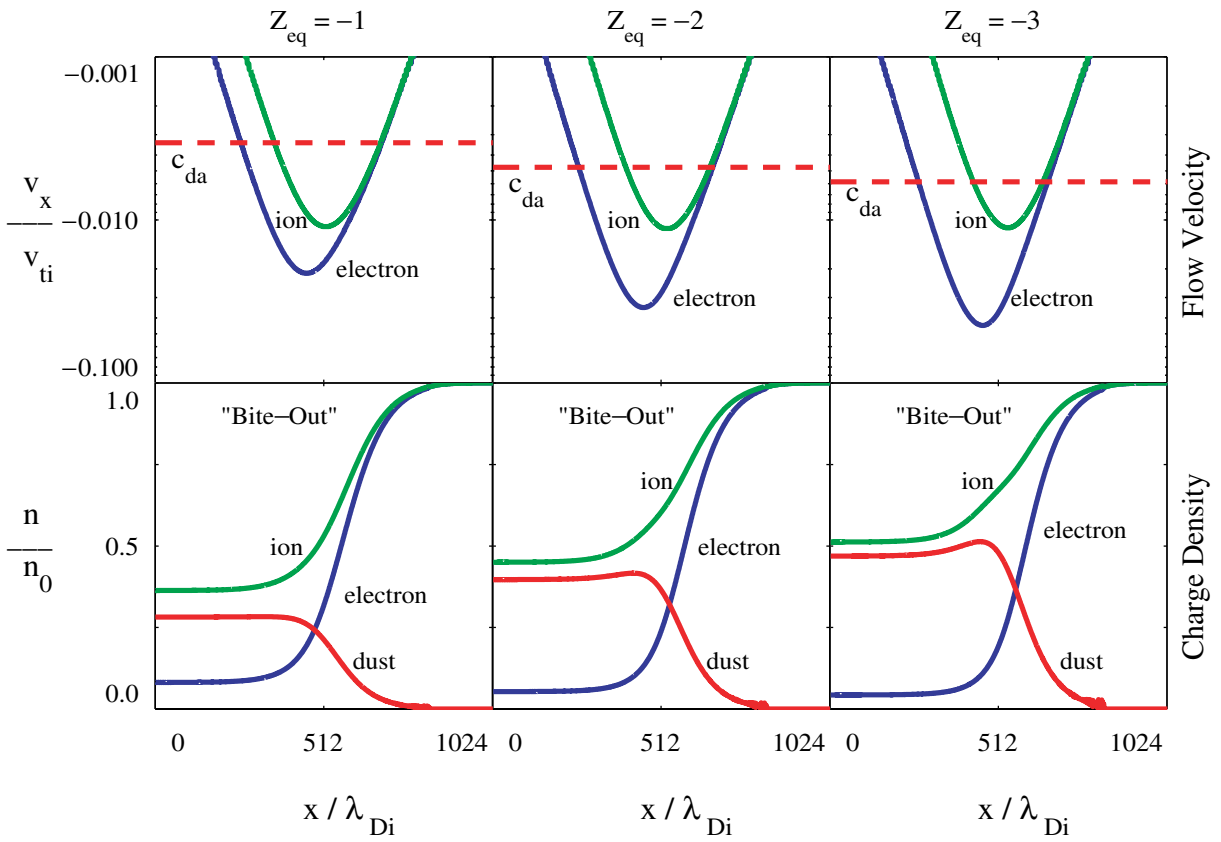

Figure 3. Behaviour of normalized plasma flows and densities in the steady-state charged dust cloud boundary layer with varied equilibrium charge Z_{eq} and $n_{d0}/n_{e0} = 0.5$. The flows exceed the dust acoustic speed c_{da}, denoted by the dotted line.

where $\chi_{e,i,d}$ denotes the electron, ion and dust susceptibilities. For the conditions here, the electron and ions are assumed to be thermal and drifting relative to the dust; therefore, the susceptibilities are taken to be given by

$$\chi_e = \frac{1}{k_x^2 \lambda_{De}^2}\{1 + \xi_e Z(\xi_e)\}\left\{1 + \frac{i\nu_{en}}{\sqrt{2}kv_{te}} Z(\xi_e)\right\}^{-1} \tag{17}$$

and

$$\chi_i = \frac{1}{k_x^2 \lambda_{Di}^2}\{1 + \xi_i Z(\xi_i)\}\left\{1 + \frac{i\nu_{in}}{\sqrt{2}kv_{ti}} Z(\xi_i)\right\}^{-1}. \tag{18}$$

The dust is assumed to be cold and stationary; therefore, the dust susceptibility is taken to be

$$\chi_d = -\frac{\omega_{pd}^2}{(\omega(\omega + i\nu_{dn}))}. \tag{19}$$

In the expressions for the susceptibilities, $\lambda_{De,i}$ is the electron (ion) Debye length, ω_{pd} the dust plasma frequency, Z the Fried–Conte plasma dispersion function and

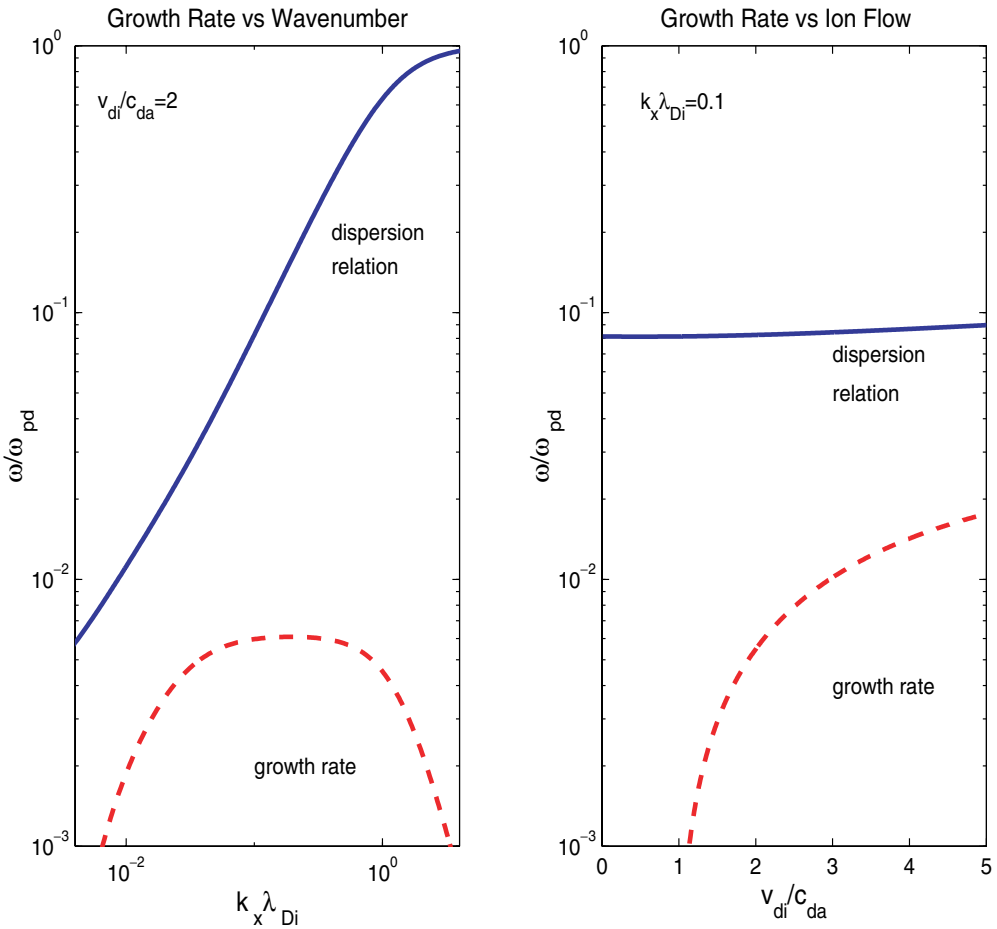

Figure 4. Growth rate calculations of dust acoustic waves for ion flow relative to the charged dust with parameters typical of the model in section 2. Note a broad spectrum of wavelengths may be excited.

$\xi_{e,i} = (\omega - k_x v_{de,i} + i\nu_{e,in})/\sqrt{2}k_x v_{te,i}$. This form of dispersion relation has been used extensively in the past to investigate dust acoustic-type plasma instabilities (see [36] and references therein). The electron and ion flows seen in figures 2 and 3 exceed the dust acoustic speed c_{da} but they are less than the ion thermal velocity v_{ti}. Therefore, the flows themselves would not be expected to drive ion waves or waves of higher frequency in the dust cloud boundary. However, dust acoustic waves may be generated in the charged dust cloud boundary since the electron and ion flows are typically several times c_{da} which is consistent with extensive earlier work on dust acoustic wave instability theory [36]. Figure 4 shows a numerical solution of the linear growth rate from (16) for parameters in the model results. Note that ν_{dn} is taken to be zero in the calculations here and this point will be discussed shortly. The variation of the growth rate with wavenumber as well as ion flow speed relative to the dust acoustic speed v_{di}/c_{da} is shown. The real frequency of this dust wave may be approximated by the well-known expression

$$\omega_r \approx \frac{k_x c_{da}}{(1 + k_x^2 \lambda_{Di}^2)^{1/2}}. \tag{20}$$

It is observed that the maximum growth rate is of the order of $0.01\omega_{pd}$ and the frequency of the waves are of the order of ω_{pd}. It is interesting that the dust plasma frequency may be estimated to be of the order of 10 Hz in this altitude regime and waves in this frequency range were observed during recent *in situ* experiments [12]. It can be noted that a relatively broad spectrum of wavenumbers is unstable with maximum growth near $k_x\lambda_{Di} \sim 0.1$. It is important to compare this spectrum with the experimental frequency spectrum observations of PMSEs. The frequency spectrum of PMSEs is quite broad from MHz to GHz with particularly strong scattering in the 50 MHz range. If one considers scattering from the plasma irregularities, one may use the Bragg scattering condition to estimate the frequency of radar scatter from a particular scale-size irregularity. The Bragg condition implies that the relationship between the radar scatter and irregularity wavelengths is $\lambda_{radar} = 2\lambda_{irregularity}$. Therefore, the scale size of irregularities to produce PMSEs should be in the range from 10 m to 10 cm with scattering particularly strong in the metre to sub-metre range. The wavelength of irregularities in figure 4 is quite broad with roughly $0.01 < k_x\lambda_{Di} < 1$. For an ion Debye length of the order of centimetres, this implies irregularities from roughly metre scale sizes to 10 cm, which is consistent with the experimental observations. The variation of growth rate with relative ion-dust drift indicates the increase in growth rate when $v_{di} > c_{da}$. In the case of the model calculation in the previous section, $v_{di} \approx 2c_{da}$ or larger.

It can be shown from numerical solution of (16) that electron flows of the magnitude indicated in figures 2 and 3 may destabilize dust acoustic waves as well. It is found that for typical electron flows observed in the model equilibrium boundary layer, this process is much less efficient than the production of dust acoustic irregularities by the ion flow. However, it is observed that the electron flows may produce a beam–plasma interaction, which will lead to irregularities in the dust wave regime that have more substantial growth rates. These waves have a real wave frequency which may be roughly approximated by

$$\omega \sim k_x v_{de}. \tag{21}$$

Figure 5 shows numerical calculations of the dispersion relation and growth rate of irregularities due to the electron flow. The electron flow in figures 2 and 3 may be in the range of $2–30c_{da}$. In the calculation of the growth rate with wavenumber k_x in figure 5, $v_{de}/c_{da} = 20$. It can be seen that irregularities are driven unstable with $k_x\lambda_{Di} \sim 0.01$ and growth rate of the order of $0.01\omega_{pd}$. From the Bragg condition, these waves would have the appropriate spatial scales in the range believed to produce PMSEs. It can be seen from figure 5 that the electron flow may possibly be an effective way of producing irregularities when $v_{de}/c_{da} > 5$.

There are several considerations to the applicability of the present irregularity generation analysis. The first is the lifetime of the dust boundary. This is of course determined by the dust diffusion time. This has been recently extensively investigated [7, 8]. The dust diffusion time may be approximated by

$$\tau_{diff} \approx \frac{m_d \nu_{dn}}{KT} \ell^2, \tag{22}$$

where recall ℓ is the scale length of the boundary layer. For typical quantities, this time is predicted to be of the order of 10^4 s. This is much longer than the characteristic dust plasma time scale as described earlier; therefore, dust irregularities may grow within the lifetime of the boundary. Another important consideration is the collisionality of the dust. If the standard hard

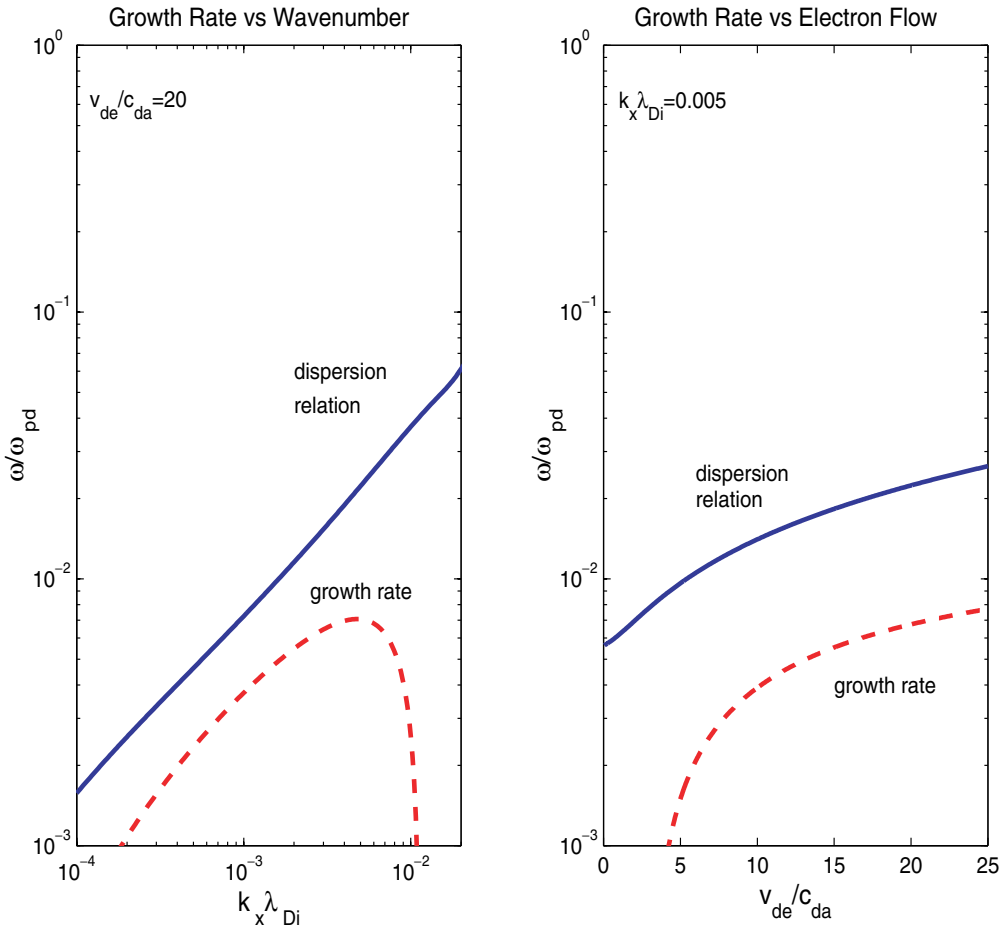

Figure 5. Growth rate calculations for beam–plasma interaction waves in the dust regime due to electron flow relative to ions and charged dust.

sphere model is used to calculate the dust-neutral collision frequency [23] then

$$\nu_{\mathrm{dn}} \approx r_{\mathrm{d}}^2 n_{\mathrm{n}} \frac{m_{\mathrm{n}}}{m_{\mathrm{d}}} v_{\mathrm{tn}}, \tag{23}$$

where n_{n}, m_{n} and v_{tn} are the neutral density, mass and thermal velocity, respectively. Using typical values, $n_{\mathrm{n}} \sim 10^{20}\,\mathrm{m}^{-3}$, $m_{\mathrm{d}}/m_{\mathrm{n}} \sim 10^5$ and $T = 150\,\mathrm{K}$, yields $\nu_{\mathrm{dn}} \sim 100\,\mathrm{Hz}$ which compares with $\omega_{\mathrm{pd}} \sim 10\,\mathrm{Hz}$. Therefore, the standard homogenous dust acoustic instability discussed would not yield unstable waves under these circumstances. Therefore, the fact that the flows and densities are inhomogenous in the boundary region must ultimately be considered for a complete and accurate plasma instability analysis. Many of the crucial dust parameters are not particularly well determined and more investigation is required. The electric field in the charged dust boundary as well as the plasma flows depend on a variety of parameters such as the dust radii, plasma temperatures, relative plasma and aerosol densities and collisions. A much more thorough parametric study is required before definite conclusions can be made here and the current results should be taken to be preliminary. However, the results here are useful in that they have provided rough estimates of the spatial and temporal scales involved.

4. Conclusions

A possible mechanism for generating dust irregularities that may ultimately produce PMSEs has been investigated. This mechanism results from plasma inhomogeneity in the boundary region between the background mesospheric plasma and the region that contains significant charged dust density. The signature of this boundary is the electron 'bite-out' which is often observed to be associated with PMSEs. The equilibrium boundary of the 'bite-out' may exhibit localized electron and ion flows into the region of plasma reduction. These steady localized flows result from the equilibrium balance between diffusion, charging, photoionization and recombination effects. The boundary flows may exceed the dust acoustic speed c_{da} for boundaries with scale lengths of tens of metres. Increasing the neutral dust density increases the flow speeds relative to c_{da}. Also, increasing the dust radius, or equivalently equilibrium charge, increases the electron flow, but produces slight decreases in the ion flow. Both the ion and electron flows may be capable of generating dust irregularities in the appropriate spatial-scale regime depending on the dust parameters. A preliminary assessment of the dust irregularities that may be generated by these localized flows was made by considering basic dust acoustic and beam–plasma streaming instabilities. Using the standard hard sphere model for dust neutral collisions predicts that the standard homogenous dust acoustic instability would be collisionally damped and therefore not yield irregularities. This indicates that the inhomogeneities in the boundary region between the background plasma and dust plasma may probably cause significant changes to the characteristics of the irregularities and must be considered. Much further investigation is required to thoroughly assess the role of these flows in producing irregularities. A more realistic model for the boundary layer waves must be developed including the effects of the inhomogeneities. Also, a wider set of parameter regimes than discussed in the present work must be considered. It must be reiterated that recent experimental observations of 10 Hz waves [12] are consistent with dust waves considered by the present model; however, the generation mechanism remains unresolved. The higher frequency kHz waves observed are outside the realm of the current irregularity analysis but possibly not the basic equilibrium model discussed here. It should be noted that recent analysis of previous experimental observations indicate that PMSEs maximize in regions of maximum $r_d^2 Z_d n_d$ [37]. For constant dust radius, this indicates that PMSEs maximize in the region of maximum dust charge density. It is interesting to note that the current model predicts that the maximum dust charge density may occur in the boundary for typical parameters and also this is the region the maximum plasma flows develop. Future work will consider the effects of a distribution of dust radii on the charged dust boundary electrodynamics. The model described here will also ultimately be used to consider irregularity temporal development and evolution on dust time scales.

Acknowledgments

This work was supported by the National Science Foundation under grant ATM0234062 and the Office of Naval Research.

References

[1] Cho J Y N and Kelley M C 1993 *Rev. Geophys.* **31** 243
[2] Cho J Y N and Rottger J 1997 *J. Geophys. Res.* **102** 2001

[3] Czechowsky P, Ruster R and Schmidt G 1979 *Geophys. Res. Lett.* **6** 459
[4] Eklund W L and Balsley B B 1981 *J. Geophys. Res.* **86** 7775
[5] Kelley M C and Ulwick J C 1988 *J. Geophys. Res.* **93** 7001
[6] Havnes O, Troim J, Blix T, Mortensen W, Naesheim L K, Thrane E and Tonnesen T 1996 *J. Geophys. Res.* **101** 10839
[7] Rapp M and Lubken F-J 2003 *J. Geophys. Res.* **108** 8437
[8] Lie-Svendsen O, Blix T A and Hoppe U-P 2003 *J. Geophys. Res.* **108** 8442
[9] Dimant Y S and Sudan R N 1995 *J. Geophys. Res.* **100** 14605
[10] Blix T A, Thrane E V, Kirkwood S, Dimant Y S and Sudan R N 1996 *Geophys. Res. Lett.* **23** 2137
[11] Blix T A 1999 *Adv. Space Res.* **24** 537
[12] Pfaff R *et al* 2001 *Geophys. Res. Lett.* **28** 1431
[13] Ganguli G, Bernhardt P, Scales W, Rodriguez P, Siefring C and Romero H 1993 Physics of negative ion plasmas created by chemical releases in space *Physics of Space Plasmas* vol 12, ed T Chang (SPI Conf. Proc. and Reprint Series) (Cambridge, MA: Scientific Publishers Inc.) p 161
[14] Scales W, Bernhardt P, Ganguli G, Siefring C and Rodriguez P 1994 *Geophys. Res. Lett.* **21** 605
[15] Goldberg R A *et al* 2001 *Geophys. Res. Lett.* **28** 1407
[16] Hunten D M, Turco R P and Toon O B 1980 *J. Atmos. Sci.* **37** 1342
[17] Havnes O, Aslaksen T and Brattli A 2001 *Phys. Scripta* **T89** 133
[18] Havnes O, Brattli A, Aslaksen T, Singer W, Latteck R, Blix T, Thrane E and Troim J 2001 *Geophys. Res. Lett.* **28** 1419
[19] Birdsall C K and Langdon A B 1991 *Plasma Physics via Computer Simulation* (New York: McGraw-Hill)
[20] Shukla P K and Mamun A A 2002 *Introduction to Dusty Plasma Physics* (Philadelphia, PA: Institute of Physics)
[21] Winske D and Rosenberg M 1998 *IEEE Trans. Plasma Sci.* **26** 92
[22] Hill R J 1978 *J. Geophys. Res.* **83** 989
[23] Cho J Y N, Hall T M and Kelley M C 1992 *J. Geophys. Res.* **97** 875
[24] Reid G C 1990 *J. Geophys. Res.* **95** 13891
[25] Rapp M and Lubken F-J 2001 *J. Atmos. Solar Terr. Phys.* **63** 759
[26] Natanson G L 1960 *Sov. Phys. Tech. Phys. (Engl. Transl.)* **5** 538
[27] Bernstein I B and Rabinowitz I N 1959 *Phys. Fluids* **2** 112
[28] Chen F F 1965 *Plasma Phys.* **7** 47
[29] Zadorozhny A M, Tyutin A A, Witt G, Wilhelm N, Walchli U, Cho J Y N and Swartz W E 1993 *Geophys. Res. Lett.* **20** 2299
[30] Zadorozhny A M 2000 *Geophys. Res. Lett.* **27** 493
[31] Holzworth R H *et al* 2001 *Geophys. Res. Lett.* **28** 1435
[32] Pfaff R, Goldberg R A, Maynard N C, Witt G and Hale L 1988 *EOS Trans. Am. Geophys. Union* **69** 1339
[33] Goldberg R A 1989 *J. Geophys. Res.* **94** 14661
[34] Scales W A, Bernhardt P A and Ganguli G 1995 *J. Geophys. Res.* **100** 269
[35] Ichimaru S 1973 *Basic Principles of Plasma Physics* (Reading, MA: Benjamin-Cummings)
[36] Rosenberg M 1993 *Planet. Space Sci.* **41** 229
[37] Rapp M, Lubken F, Hoffmann P, Latteck R, Baumgarten G and Blix T 2003 *J. Geophys. Res.* **108** 8441